

ELECTRIC FIELD GRADIENTS IN MgB₂ SYNTHESIZED AT HIGH PRESSURE: ¹¹¹Cd TDPAC STUDY AND *AB INITIO* CALCULATION

A.V. Tsvyashchenko^{a,*}, L.N. Fomicheva^a, M.V. Magnitskaya^a, E.N. Shirani^a,
V.B. Brudanin^b, D.V. Filossofov^b, O.I. Kochetov^b, N.A. Lebedev^b, A.F. Novgorodov^b
A.V. Salamatin^b, N.A. Korolev^b, A.I. Velichkov^b, V.V. Timkin^b,
A.P. Menushenkov^c, A.V. Kuznetsov^c, V.M. Shabanov^c and Z.Z. Akselrod^d

^a Institute for High Pressure Physics, 142190 Troitsk, Moscow Region, Russia

^b Joint Institute for Nuclear Research, 141980 Dubna, Moscow Region, Russia

^c Moscow Engineering-Physics Institute, 115409 Kashirskoe shosse 31, Moscow, Russia

^d Institute of Nuclear Physics, Moscow State University, 119899 Vorob'evy gory, Moscow, Russia

Abstract

We report the high-pressure synthesis of novel superconductor MgB₂ and some related compounds. The superconducting transition temperature of our samples of MgB₂ is found to be 36.6 K. The MgB₂ lattice parameters determined via X-ray diffraction are in excellent agreement with results of our *ab initio* calculations. The TDPAC measurements of ¹¹¹Cd quadrupole frequency ν_Q demonstrate a small increase in ν_Q with decreasing temperature from T_{room} to T_{He} . The electric field gradient V_{zz} at the B site calculated from first principles is in fair agreement with V_{zz} obtained from ¹¹B NMR spectra of MgB₂ reported in the literature. It is also very close to V_{zz} found in our ¹¹¹Cd TDPAC experiments, which suggests that the ¹¹¹Cd probe substitutes for boron in the MgB₂ lattice.

1. INTRODUCTION

The recent discovery of intermediate-temperature superconductivity in magnesium diboride MgB₂ with $T_c \sim 39$ K¹ and its almost simultaneous explanation in terms of phonon-mediated BCS superconductivity based on the observation of significant boron isotope effect² has triggered an avalanche of theoretical work including *ab initio* electronic band structure calculations (see, e.g.^{3,4,5,6}). A recent ¹¹B NMR study⁷ has revealed an exponential temperature dependence of the nuclear relaxation rate $1/T_1$ in the superconducting (SC) state, with a relatively large SC gap of $2D/k_B T_c \sim 5$ implying strong-coupling s-wave superconductivity in this system. Other ¹¹B NMR studies^{8,9} of MgB₂ have provided important information on the local electronic state of the boron

* Fax: (7-095) 334-0012; E-mail: tsvyash@ns.hppi.troitsk.ru

site by measuring the ^{11}B quadrupole coupling constant $\mathbf{n}_Q = eQV_{zz}/h$ that can be evaluated theoretically from first-principles calculations.

In NMR experiments, however, the resonance frequency of ^{11}B is determined both by the hyperfine magnetic interaction and by the hyperfine interaction of the ^{11}B quadrupole moment Q with electric field gradient (EFG) V_{zz} , created at the boron site by electronic and ionic environment. This combined interaction complicates the determination of \mathbf{n}_Q . For instance, Tou *et al.*¹⁰ have found that in the normal state ($T = 50$ K) \mathbf{n}_Q obtained from magnetic-field dependence of the NMR frequency shift is equal to 1100 ± 150 kHz. However, $\mathbf{n}_Q(\text{FWHM})$ determined through the relation $\mathbf{n}_Q(\text{FWHM}) = 1.3856(\mathbf{n}_0\Delta\mathbf{n})^{1/2}$, where $\Delta\mathbf{n}$ is the width between the peak and shoulder of NMR spectrum, is equal to 835 kHz¹⁰, in close agreement with the \mathbf{n}_Q values found in other NMR experiments^{8,9} (see Table 2 below).

In this paper, the results of high-pressure synthesis of MgB_2 , as well as of some related compounds are presented. We use the time-differential perturbed angular $\gamma\gamma$ -correlation (TDPAC) method to investigate the hyperfine quadrupole interaction at ^{111}Cd probe nucleus in the MgB_2 lattice consisting of alternating graphite-like layers of B atoms and hexagonal layers of Mg atoms, with axial symmetry of electric field gradients. Previously, this high-pressure technique has been successfully applied, e.g., for synthesis of high-pressure phases of YbFe_2 with subsequent ^{111}Cd TDPAC investigation of these phases¹¹. In contrast to the NMR experiments, this PAC method allows to determine \mathbf{n}_Q in MgB_2 directly, since there is no hyperfine magnetic interaction on the ^{111}Cd nucleus, owing to the lack of magnetic ordering in MgB_2 . We present also *ab initio* band-structure calculations of EFG's at the B and Mg atoms in MgB_2 and compare these results with our experimental data.

2. HIGH-PRESSURE SYNTHESIS

Magnesium diboride samples were prepared by reacting stoichiometric amounts of powdered B and Mg at constant temperature $T \geq 900^\circ\text{C}$ and constant pressure of 6 ~ 8 GPa in a high-pressure "Toroid" cell constructed by Khvostantsev *et al.*¹². Two different experimental techniques were applied. At first, the pellet was prepared by compacting the well-mixed powdered constituents at room temperature. With the first technique of solid-phase synthesis, the pellet was placed into the tantalum heater where it was held for 20 – 40 min at the constant pressure of 6.2 GPa and temperature of 950°C which is lower than T_{melt} of Mg at this pressure¹³. In this case, temperature was controlled by a chromel-alumel thermocouple located outside the heater near its wall. In the second case, the pellet was placed in a rock-salt pipe ampoule and then directly heated

electrically to $T \sim 1500^\circ\text{C}$ (above T_{melt} of Mg) at a constant pressure in the range $6 < p < 8$ GPa. In the both cases the experimental sample was then rapidly quenched to room temperature, and pressure was released. The structural properties of the samples obtained with both techniques were found to be identical, and their SC properties are also quite similar.

After high pressure–high temperature treatment, the samples were investigated at normal conditions. The structure and phase composition of the samples obtained were determined from X-ray powder patterns with a 114-mm camera RKU-114 and Cu K_α radiation. X-ray analysis showed that at ambient conditions the MgB_2 samples have the hexagonal AlB_2 -type structure, space group $\text{P6}/\text{mmm}$, and lattice parameters $a = 3.075\text{\AA}$, $c = 3.519\text{\AA}$, $c/a = 1.144$. A weak trace of MgO was also observed in the powder patterns. AC susceptibility measurements showed the SC transition with $T_c = 36.6$ K. The results of these measurements are presented in Fig. 1.

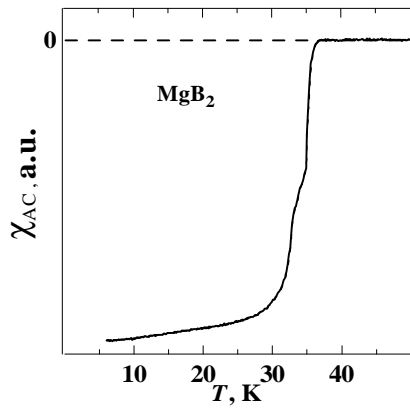


Fig.1. Magnetic susceptibility of MgB_2 as a function of temperature.

It should be mentioned that we synthesized also the compounds BeB_2 , CaB_2 and $\text{Ca}_{0.5}\text{Mg}_{0.5}\text{B}_2$ using the same high-pressure technique. All these three alloys do not belong to the AlB_2 -type structure and are not superconducting up to 4.2 K. Our results on BeB_2 agree with other investigations of this compound¹⁴.

Besides, we synthesized compounds in the systems $\text{Mg}(\text{B}_{1-x}\text{Ga}_x)_2$ at $0.05 \leq x \leq 1.0$ and $\text{Mg}_{1-x}\text{Sc}_x\text{B}_2$ at $0 \leq x \leq 0.3$. The substitution of Mg with Sc was found to reduce T_c considerably, but the AlB_2 -type crystal structure remains unchanged. Similar results have been obtained by

other groups investigating the substitution of Mg with Al¹⁵ and Li¹⁶. In turn, the replacement of B with Ga reduces T_c as well, which correlates with the results of other experiments¹⁷ on boron sublattice doping. In this series of experiments, however, a single phase of composition close to MgBGa was synthesized, which possessed $T_c = 32$ K. At normal conditions this high-pressure phase is rather unstable — it breaks down to the mixture of powdered MgB_2 and MgGa_2 in a few days. The crystal structure of MgBGa was tentatively determined as cubic SrSi_2 -type structure (perhaps, distorted) with lattice parameter $a = 6.291\text{\AA}$. In this context, we would like to mention the recent work by Sanfilippo *et al.*¹⁸ who observed superconductivity with $T_c = 14$ K in high-pressure phase of CaSi_2 (AlB_2 -type structure) at $p = 16$ GPa. It should be noted that various low-pressure and high-pressure phases of both disilicides, CaSi_2 and SrSi_2 , are characterized by 3-connected nets of Si¹⁹.

3. TDPAC MEASUREMENTS

^{111}In was produced via the reaction $^{109}\text{Ag}\{\alpha, 2n\}^{111}\text{In}$ by irradiation of a metallic silver target with α particles ($\dot{A}_\alpha = 30$ MeV) at the U-200 cyclotron of JINR, Dubna. $^{111}\text{In}^{20}$ of high specific activity was diffused into the MgB_2 samples at 550°C for 2.5 hrs. The thermal diffusion proceeded in vacuum to prevent oxidation, and a tantalum sample holder was used. The excited state (spin $I = 7/2^+$, energy $E = 420$ keV) of ^{111}Cd populated via the electronic-capture decay of ^{111}In de-excites, by way of the $\gamma\gamma$ -cascade of 171–245 keV, to the ground state ($I = 1/2^+$) through the isomeric intermediate state of ^{111}Cd with $I = 5/2^+$, $E = 247$ keV, half-period $t_{1/2} = 85$ ns and nuclear quadrupole moment $Q = +0.83(13)$ b²¹. The angular correlation of this cascade is largely anisotropic ($\dot{A}_2^{\text{max}} = -18.0\%$).

A four-detector TDPAC spectrometer, with detectors arranged in a plane at 90° angular intervals and controlled by a personal computer has been developed²² for detecting PAC at different temperatures and pressures. The four NaI(Tl) cylindrical detectors (40x40 mm) coupled to the Philips XP2020Q photomultipliers provide the time resolution of 2.5 ns (FWHM) per detector pair for $\gamma\gamma$ -cascade of 172–247 keV of ^{111}Cd . The low-temperature experiments can be performed with a nitrogen cryostat.

The components of the EFG tensor referred to its principal axes are denoted as V_{xx} , V_{yy} and V_{zz} . In the case of hexagonal MgB_2 lattice, the coordinate axes are chosen such that V_{zz} is the EFG component along the crystallographic c axis and $|V_{zz}| > |V_{yy}| \geq |V_{xx}|$. Then the EFG tensor is completely characterized by two parameters: the largest component V_{zz} and the axial asymmetry parameter h defined as $h = |V_{xx} - V_{yy}| / |V_{zz}|$.

Data processing aimed at the determination of these parameters starts with calculation of a ratio $R(t)$ from the experimental spectra $N(\mathbf{J}, t)$:

$$R(t) = -2[N(180^\circ, t) - N(90^\circ, t)]/[N(180^\circ, t) + 2N(90^\circ, t)] \quad .$$

For polycrystalline samples, with the assumption of a Lorentzian distribution of EFG, theoretical calculations^{23,24} give

$$R(t) = \dot{A}_{22}^{\text{eff}} \sum_n s_{2,n} \cos(a_n \mathbf{w}_0 t) \exp(-a_n \mathbf{L} t) \quad ,$$

where \mathbf{w}_0 is the quadrupole frequency, $\mathbf{w}_0 = 3\pi |eQV_{zz}/h| / I(2I-1)$ for half-integral spin I . The frequency \mathbf{w}_0 is a function of the quadrupole coupling constant $\mathbf{n}_Q = eQV_{zz}/h$. Here Q is the nuclear quadrupole moment for ^{111}Cd intermediate state of γ -ray cascade, h is the Planck's

constant and L is a relative width of the quadrupole frequency distribution due to lattice defects and other imperfections. The coefficients a_n and $s_{2,n}$ depend on n and \mathbf{h}^{24} . For $\mathbf{h} = 0$, a_n is equal to n , resulting in a periodic R -vs.- t pattern.

In Figure 2, the TDPAC spectra taken both at room temperature (a) and at $T = 143$ K (b) are displayed. The least-squares fits of the theoretical relation $R(t)$ to the experimental data were obtained by means of an appropriate MATLAB routine.

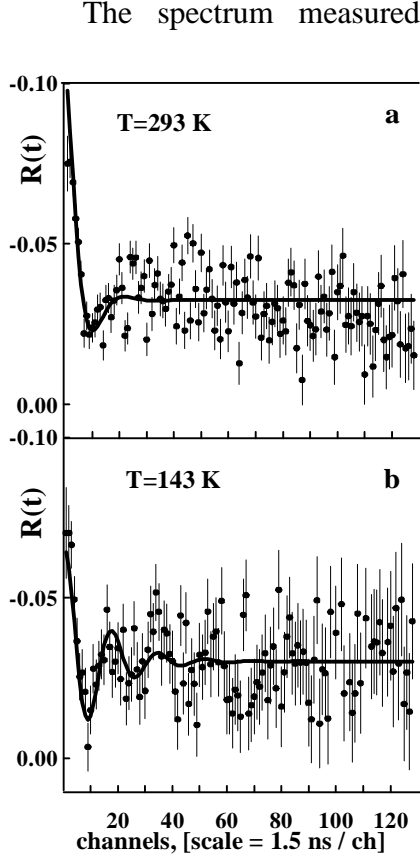


Fig. 2. ^{111}Cd TDPAC spectra for MgB_2 at two temperatures. The solid curves are the fits of $R(t)$ to the experimental data.

The spectrum measured at room temperature is characterized by a nonperiodic perturbation corresponding to a rather broad distribution of the quadrupole frequency with an average value of \mathbf{n}_Q equal to 31.0(1) MHz and $L = 0.12$, which gives $V_{zz} = 15.4 \times 10^{16}$ V/cm 2 . The spectrum taken at $T = 143$ K is characterized by a periodic perturbation corresponding to a smaller distribution of the quadrupole frequency, with the average equal to 37.5(1) MHz and $L = 0.05$, which gives $V_{zz} = 18.6 \times 10^{16}$ V/cm 2 .

Thus, the quadrupole coupling constant \mathbf{n}_Q (and, correspondingly, V_{zz}) decreases with increasing temperature. This result does not contradict to the well-known law of $T^{3/2}$ applicable mainly to the probe nuclei of sp elements 23 , $\mathbf{n}_Q(T) = \mathbf{n}_Q(0)(1 - BT^{3/2})$, where $\mathbf{n}_Q(0)$ is the quadrupole coupling constant at 0 K. For MgB_2 , the value of parameter B obtained by fitting the $\mathbf{n}_Q(T)$ law to the experimental data is $B \sim 4.8 \times 10^{-5}$ K $^{-3/2}$. This formula extrapolated from the normal state to lower temperatures gives an estimate $\mathbf{n}_Q(0) \sim 40.9$ MHz, corresponding to $V_{zz} \sim 20.3 \times 10^{16}$ V/cm 2 .

4. AB INITIO CALCULATIONS

We calculated the electronic band structure and ground-state (i.e. at $T = 0$ K) properties of MgB_2 within density functional theory 25 using the full-potential linearized augmented plane wave (FPLAPW) method as implemented in the WIEN97 code 26 , with the generalized gradient approximation (GGA) 27 for the exchange-correlation potential. The muffin-tin radii of Mg and B equal to 1.8 and 1.5 a.u., respectively, were kept constant on varying both the volume and c/a . The

mesh of 162 \mathbf{k} -points was used in the irreducible wedge of the Brillouin zone. The Mg 2s and 2p states were treated as band states using the local orbital extension of the LAPW method²⁸. Parameters of our calculation were as follows: the potential and the charge density were expanded up to $l_{\max} = 10$ and $g_{\max} = 15$ a.u.⁻¹, the cutoff $r_{\text{MT}}k_{\max}$ was chosen to be equal to 8.0.

Total energy was calculated as a function of unit cell volume W over the range $(0.88 - 1.09)W_{\text{exp}}$, where W_{exp} is the experimental equilibrium volume at normal pressure. At each value of W , the c/a ratio was optimized. An energy-vs.-volume relation obtained by integrating the Birch $p(W)$ equation of state²⁹ was fitted to the calculated values of $E(W)$ to find the theoretical equilibrium volume $W_{\text{teor}} = 1.002W_{\text{exp}}$, the bulk modulus K and its pressure derivative K' (see Table 1 below) The lattice parameters a , c and c/a determined in this work are presented in Fig. 3, where the experimental results by Vogt *et al.*⁵ are also plotted for comparison.

5. DISCUSSION

Table 1 presents the MgB₂ lattice parameters determined in this work, as well as those measured by various groups^{2,5,30,31} and calculated from first principles^{3,4,5,6}. As is evident from Table 1, almost all the experimental and theoretical lattice parameters, a and c , are in very good agreement with each other (note the coincidence of our theoretical lattice parameters with those calculated in Ref. ⁴ using the same WIEN97 code). However, the more sensitive c/a ratio obtained in all the calculations is systematically slightly higher than c/a measured experimentally. Among the experimental lattice parameters, the lowest a , c and the highest c/a are observed for our samples synthesized at a constant high pressure in the range 6 – 8 GPa. A noticeable spread in lattice parameters measured by various groups for samples obtained at different conditions may be ascribed to an appreciable non-stoichiometry, namely, a possible deficit either in Mg or in B. Notice that the ambient-pressure synthesis at $\dot{O} \sim 900 - 950^\circ\text{C}$ (see, e.g. Ref. [2]) might lead to the essential sublimation of magnesium (at $p = 0$, T_{melt} of Mg is equal to 650°C), with the resultant deficit in Mg. On the other hand, according to Pearson³², a deficit in B is practically unavoidable in MgB₂. It should be emphasized, however, that at the high-pressure synthesis of MgB₂, the

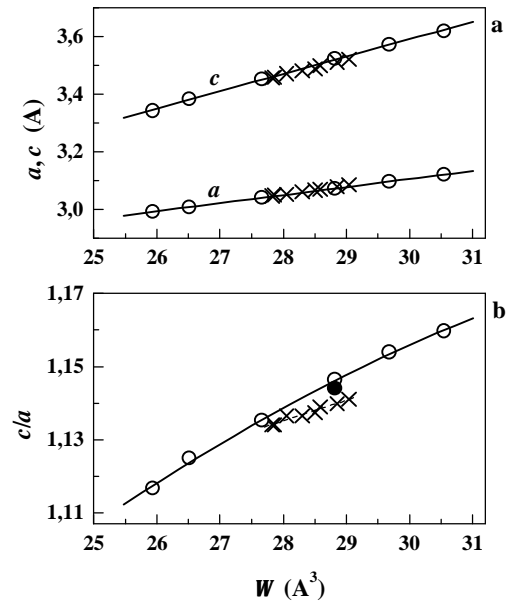


Fig. 3. Volume dependence of the lattice parameters (a) and c/a ratio (b) of MgB₂. The c/a value measured in this work is denoted with solid circle. The open circles and the crosses represent the results of our calculations and the experimental data⁵, respectively.

sublimation of either element is impossible, because (i) T_{melt} and T_{subl} of parent substances increase with increasing pressure¹³ and (ii) the reaction proceeds in closed space.

Table 1. Theoretical and experimental information on structural and mechanical properties of MgB₂ at normal conditions

Reference	a (Å)	c (Å)	c/a	B (GPa)	B'
Experiment					
[2]	3.140	3.520	1.121		
[5]	3.086 3.048 ^a	3.521 3.457 ^a	1.141 1.134 ^a	151±5	4
[30]	3.085 3.082 ^b	3.521 3.515 ^b	1.141 1.140 ^b	146.8	
[31]	3.084	3.523	1.142		
Present	3.075	3.519	1.144		
Theory					
Present	3.075	3.527	1.147	142.6	3.46
[4]	3.075	3.527	1.147	140.1	3.93
[6]	3.065	3.519	1.148		
[3]	3.071	3.528	1.149		
[5]	3.089	3.548	1.149	139	

^a $p = 8$ GPa.

^b $T = 37$ K.

the stoichiometry of MgB₂. The analysis of various experimental and theoretical results on MgB₂ implies that the thorough investigation of its superconducting and other physical properties requires either the obtaining of polycrystalline samples with composition controlled to high accuracy or the growth of MgB₂ single crystals.

The superconducting transition temperature measured for our MgB₂ samples synthesized at high pressure is $T_c \sim 36.6$ K, which is slightly lower than $T_c \sim 39$ K found by other groups. This corresponds to a decrease in T_c with decreasing volume (increasing pressure), which was observed for MgB₂ samples synthesized at normal pressure^{31,33}.

While the quadrupole frequency determined in our ¹¹¹Cd TDPAC measurements increases with decreasing temperature, no temperature dependence of n_Q (FWHM) was observed in the ¹¹B NMR experiments⁹. This fact, together with the large (> 30%) discrepancy between the n_Q values

determined by two different ways in Ref.¹⁰, points out that the temperature dependence of V_{zz} cannot be established reliably in NMR experiments.

The calculated values of EFG's at the B è Mg sites of MgB_2 are displayed in Table 2. As is seen from the table, V_{zz} on the B site is about one order of magnitude higher than V_{zz} at the Mg site and is opposite in sign. The value of EFG at the B site is in reasonable agreement with EFG's

Table 2. EFG's V_{zz} ($10^{16} \times \text{V}/\text{cm}^2$) obtained both from our TDPAC measurements and from the NMR experiments in comparison with our theoretical results

Site		Mg	B
Calculation		-3.2	18.5
^{111}Cd PAC	T_{room}		15.4
	143 K		18.6
	0 K ^a		20.3
^{11}B NMR	[8]		16.8
	[9]		17.0±0.1
			17.0±1
	[10]		22.4±3 ^b

^a Extrapolation to $T = 0$.

^b Determined from field dependence.

obtained from ^{11}B NMR spectra^{8,9,10}. As for V_{zz} at the Mg site, no ^{25}Mg NMR measurements have been made for MgB_2 so far, which could provide relevant experimental information.

In the process of thermal diffusion, ^{111}In — a parent isotope for ^{111}Cd — could replace both the Mg and B atoms in the MgB_2 lattice. Indium is isovalent to boron, but its atomic radius is comparable with that of Mg. Considering that the experimental EFG obtained from our ^{111}Cd TDPAC measurements of n_Q is close to calculated V_{zz} at the B site, we suppose that in our experiments, ^{111}In probe falls into the B site of MgB_2 lattice. Probably, a broad distribution of quadrupole frequencies observed in the TDPAC spectra reflects a large degree of disorder occurring around the $^{111}\text{In}/^{111}\text{Cd}$ probe because of

considerable difference in size between B and In/Cd atoms.

To conclude, our high-pressure technique was applied for synthesis of MgB_2 . We consider this method to be capable of producing MgB_2 samples close to stoichiometry. The value of EFG at the B site, obtained in this work both from *ab initio* calculations and from ^{111}Cd TDPAC experiments, agrees rather well with those determined from ^{11}B NMR spectra. In contrast to the NMR experiments, our TDPAC measurements show that n_Q and, correspondingly, V_{zz} increase as temperature decreases from room temperature to $T = 4$ K.

Acknowledgements—We are grateful to E.G. Maksimov for valuable discussions and to A. Werbel for providing the setup for thermal diffusion. The work was supported by the Russian Foundation for Basic Research, Grant 99-02-17897. M.V. Magnitskaya acknowledges partial financial support from International Science and Technology Center under project No. 207.

REFERENCES

-
- ¹ J. Nagamatsu, N. Nakagawa, T. Muranaka, Y. Zenitani, J. Akimitsu, *Nature* **410** (2001) 63.
- ² S.L. Bud'ko, G. Lapertot, C. Petrovic, C.E. Cunningham, N. Anderson, P.C. Canfield, *Phys. Rev. Lett.* **86**, 2001, 1877.
- ³ J. Kortus, I.I. Mazin, K.D. Belashchenko, V.P. Antropov, L.L. Boyer, *Phys. Rev. Lett.* 2001 (in press); cond-mat/0101446.
- ⁴ I. Loa, K. Syassen, *Solid State Commun.*, 2001 (in press); cond-mat/0102462.
- ⁵ T. Vogt, G. Schneider, J.A. Hriljac, G. Hriljac, J.S. Abell, cond-mat/0102480.
- ⁶ J.B. Neaton, A. Perali, cond-mat/0104098.
- ⁷ H. Kotegawa, K. Ishida, Y. Kitaoka, T. Muranaka, J. Akimitsu, cond-mat/0102334.
- ⁸ A. Gerashenko, K. Mikhalev, S. Verkhovskii, cond-mat/0102421.
- ⁹ J.K. Jung, Seung Ho Baek, F. Borsa, S.L. Bud'ko, G. Lapertot, P.C. Canfield, cond-mat/0103040.
- ¹⁰ H. Tou, H. Ikejiri, Y. Maniwa, T. Ito, T. Takenobu, K. Prassides, Y. Iwasa, cond-mat/0103484.
- ¹¹ B.A. Komissarova, G.K. Ryasny, A.A. Sorokin, L.G. Shpinkova, A.V. Tsvyashchenko, L.N. Fomicheva, *Phys. Status Solidi B* **213**, 1999, 71.
- ¹² L.G. Khvostantsev, L.F. Vereshchagin, A.P. Novikov, *High Temp. High Press.* **9**, 1977, 637.
- ¹³ J.K. Kennedy, R. Newton, in: *Solids under Pressure* (Ed. W. Paul, D.M. Warschauer) McGraw-Hill, New York, 1963.
- ¹⁴ I. Felner, cond-mat/0102508; D.P. Young, P.W. Adams, J.Y. Chan, F.R. Fronczek, cond-mat/0104063.
- ¹⁵ J.S. Slusky, N. Rogado, K.A. Regan, M.A. Hayward, P. Khalifah, T. He, K. Inumaru, S. Loureiro, M.K. Haas, H.W. Zandbergen, R.J. Cava, *Nature*, **410**, 2001, 343.
- ¹⁶ Y.G. Zhao, X.P. Zhang, P.T. Qiao, H.T. Zhang, S.L. Jia, B.S. Cao, M.H. Zhu, Z.H. Han, X.L. Wang, B.L. Gu, cond-mat/0103077.
- ¹⁷ Jai Seok Ahn, Eun Jip Choi, cond-mat/0103169; Shao-ying Zhang, Jian Zhang, Tong-yun Zhao, Chuan-bing Rong, Bao-gen Shen, Zhao-hua Cheng, cond-mat/0103203; T. Takenobu, T. Ito, D.H. Chi, K. Prassides, Y. Iwasa, cond-mat/0103241.
- ¹⁸ S. Sanfilippo, H. Elsinger, M. Nuões-Regueiro, O. Laborde, S. LeFloch, M. Affronte, G.L. Olcese, A. Palenzona, *Phys. Rev. B* **61**, 2000, R3800.
- ¹⁹ A.F. Wells, *Structural Inorganic Chemistry*, Oxford University Press, Oxford, 1982.
- ²⁰ D.V. Filossofov, N.A. Lebedev, A.F. Novgorodov, G.D. Bonchev, G.Ya. Starodub, Preprint JINR Đ6-99-282, Dubna, 1999.

-
- ²¹ P. Herzog, K. Freitag, M. Reuschenbach, H. Walitzki, *Z. Phys. A* **294**, 1980, 13.
- ²² O.I. Kochetov, A.V. Tsvyashchenko, Ya.P. Bilyalov, A.V. Zernov, A.V. Salamatin, I. Stekl, L.N. Fomicheva, *Abst. 5-th Intern. Conf. Nuclear Spectroscopic Investigations of Hyperfine Interactions (NSI-HFI-5)*, Dubna, 22–24 Sept. 1993, Moscow State Univ. "PRINT" firm, Moscow, 1993, p. 185.
- ²³ J. Christiansen, P. Heuber, R. Keitel, W. Klinger, W. Loeffler, W. Sandner, W. Witthuhn, *Z. Phys. B* **24**, 1976, 177.
- ²⁴ H. Frauenfelder, R.M. Steffen, in: *Alpha-, Beta-, and Gamma-Ray Spectroscopy* (Ed. K. Siegbahn), North-Holland, Amsterdam, 1968.
- ²⁵ P. Hohenberg, W. Kohn, *Phys. Rev. B* **136**, 1964, 864; W. Kohn, L. Sham, *Phys. Rev. A* **140**, 1965, 1133.
- ²⁶ P. Blaha, K. Schwarz, J. Luitz, WIEN97, a Full Potential Linearized Augmented Plane Wave Package for Calculating Crystal Properties, Karlheinz Schwarz, Technische Universität Wien, Wien, Austria, 1999, ISBN 3-9501931-0-4.
- ²⁷ J.P. Perdew, S. Burke, M. Ernzerhof, *Phys. Rev. Lett.* **77**, 1996, 3865.
- ²⁸ D. Singh, *Phys. Rev. B* **43**, 1991, 6388.
- ²⁹ F. Birch, *Geophys. Res.* **83**, 1978, 1257.
- ³⁰ J.D. Jorgensen, D.G. Hinks, S. Short, cond-mat/0103069.
- ³¹ R. Lorenz, R.L. Meng, C.W. Chu, cond-mat/0102264.
- ³² W.B. Pearson, *The Crystal Chemistry and Physics of Metals and Alloys*, Wiley, New York, 1972.
- ³³ T. Tomita, J.J. Hamlin, J.S. Schilling, D.G. Hinks, J.D. Jorgensen, cond-mat/0103358.